To be sure that your preprints are promptly included in the
HIGH ENERGY PHYSICS INDEX,
send them to (if possible by air mail):

DESY Bibliothek Notkestraße 85 22603 Hamburg Germany	DESY-IfH Bibliothek Platanenallee 6 15738 Zeuthen Germany

DESY 94-194
November 1994

ISSN 0418-9833

Compensating Calorimeters with Inorganic Active Media for Improved Electron Detection

Teresa Tymieniecka
Warsaw University, Warsaw, Poland

Abstract

In this paper we describe how compensating calorimeters can be modified to improve their energy resolution for electrons without degrading their energy resolution for hadrons.

1. Introduction

A series of experiments [1]-[5] and Monte Carlo studies [6] show that the best detection of hadrons is obtained with compensating calorimeters, i.e. calorimeters with equal signals, on average, for electrons and hadrons at the same energy ($e/h = 1$). The best detection means here a good energy resolution over a wide range of incident energies and a Gaussian shape of the calorimeter signal distribution for monoenergetic particles. Compensation has been obtained experimentally only in sampling calorimeters. This calorimeter structure does not provide however as good an energy resolution for electrons as is achievable with homogeneously sensitive detectors. The aim of this paper is to suggest how compensating calorimeters can be modified to improve their energy resolution for electrons.

1.1. Detection of hadrons

A basic requirement of a calorimeter design is that it is large enough to contain the shower. Then the energy resolution is dominated by fluctuations in the shower composition (*intrinsic fluctuations*) and in the detected energy (*sampling fluctuations*). An important parameter of a hadron calorimeter, directly measurable, which describes the intrinsic fluctuations is the ratio of the mean signal from an electron to that from a hadron at the same energy (the e/h-ratio). The reason is that in the first collisions in a high energy shower (E>5 GeV) about one third of the energy goes into neutral pions. This fraction is sensitive to multiplicity fluctuations and also to conversion of the deposited energy to signal which can be quite different for π^0's and for the remaining produced particles. In addition much of the incoming hadron energy is lost to nuclear breakup. For compensating calorimeters the contribution of the described fluctuations to the energy resolution is minimized [6].

In the experiments [1]-[5] compensation has been obtained through the optimal detection of neutrons which are produced abundantly in nuclear break up. Recall that the number of emitted neutrons in a nuclear reaction is roughly proportional to the energy lost to overcome the binding forces in order to release nucleons or nuclear fragments. Neutrons with a kinetic energy below 20 MeV are detected efficiently via elastic scattering on free protons in the active medium; their contribution to the calorimeter signal depends on the hydrogen content in the active and passive layers.

Some possible modifications to the compensating calorimeter design have been already examined. Hadron detection has been investigated in a nearly compensating uranium-organic scintillator calorimeter with different admixtures of copper and in a noncompensating calorimeter

of copper-scintillator [1]. The measurements indicate that a moderate copper admixture does not seriously affect the performance of the uranium calorimeter, but that with increased copper content the resolution and the response to hadrons relative to electrons approach the performance of the noncompensating copper device. Also, it has been found to be useful to install cladding, in the form of thin layers of intermediate Z material, between the high Z absorber plates and the active material. Its effect on hadron detection has been shown to be negligible in many experiments, e.g. [2], and in Monte Carlo studies, e.g. [7].

The influence of additional hydrogenous material has been investigated experimentally [8, 9] in a lead - organic scintillator compensating calorimeter [3]. The active volume of the calorimeter was decreased by one half in two different ways: once by summing the signals from every second scintillator plate [8, 9], then by removing every second scintillator plate from the stack [9]. The additional gaps in the second structure increased the energy leakage, mainly of neutrons. A similar energy resolution $\sigma_E/E \approx (60 \pm 1)\%/\sqrt{E}$ was obtained for both setups.

Monte Carlo searches for compensating structures [6, 7, 10] show that in the region of $e/h \approx 1$ the values of the e/h ratio and energy resolution vary slowly with increasing amount of absorber with respect to the active medium with lead or uranium as absorber. Therefore thin layers of added material should not affect the hadron detection.

It has been found experimentally that for electrons and hadrons the fluctuations in the detected energy are reduced by a finer sampling of the shower. This can be seen by comparing the energy resolution for two lead-organic scintillator compensating calorimeters: (i) the 'sandwich' calorimeter with 1 cm lead layers and 0.25 cm scintillating layers [3] and (ii) the 'spaghetti' calorimeter with scintillating fibers (Sc) 1 mm in diameter imbedded in lead with their volumes in the proportion Pb:Sc=4:1 [4]. The energy resolutions of $\sigma_E/E = 44\%/\sqrt{E}$ [3] and $\sigma_E/E = 33\%/\sqrt{E}$ [4] are measured for hadrons and for electrons they are $24\%/\sqrt{E}$ and $13\%/\sqrt{E}$ respectively (with E in GeV).

Balancing costs and good particle detection, a spaghetti-type structure [4] with lead as absorber and organic scintillating fibers as active media in the proportion Pb:Sc=4:1 offers a good choice of hadron calorimeter design. It provides compensation for hadrons and a time dependent signal which can be used for the separation of electrons from hadrons.

1.2. Detection of electrons

The best energy resolutions for electrons are obtained with homogeneous calorimeters. A very good energy resolution of $\sigma_E/E = 1.3\%/\sqrt{E}+0.5\%$ has been achieved for a large number of BGO crystals in a test beam [11]; the lead glass counters in the OPAL detector give an energy resolution of $\sigma_E/E = 6.3\%/\sqrt{E}+0.2\%$ [12] and for lead fluoride crystals used as Čerenkov radiators the energy resolution of $\sigma_E/E \approx 5.6\%/\sqrt{E}$ is expected for a few GeV electrons [13]. These values can be compared to $\sigma_E/E \approx 9.5\%/\sqrt{E} + 1\%$ for the lead-scintillator (4:1) calorimeter with the very fine shower sampling provided by scintillating fibers of 0.5mm in diameter[14]. The energy resolution of lead-silicon calorimeters scales as $\sigma_E/E \approx 18\%\sqrt{\tau/E}$ where τ is the number of radiation lengths of passive material interleaved between the silicon layers [15].

A sensitivity of the electron detection to layers of low Z materials in front of or behind silicon detectors has been observed in heavy absorber sampling calorimeters [15]. This is explained by the abundance of low energy electrons which are produced in the heavier absorber material and then stopped in the low Z material. A similar effect has been measured for scintillators with cladding, e.g. [2], and for tetramethylpentane (TMP) [16].

Experiments [8] show that the energy resolution for electrons in compensating calorimeters is dominated by fluctuations from the sampling character of detection. Existing measurements with electron beams in lead-organic scintillator calorimeters suggest that the energy resolution scales with the calorimeter structure as $\sigma_E/E = C/\sqrt{E} \cdot d_{Pb}^{0.67}/d_{Sc}^{0.29}$ where d_{Pb} is the thickness of the lead plates and d_{Sc} is the thickness of the scintillator plates [17]. Therefore by changing the frequency of sampling one improves the precision of the energy measurement for electrons.

2. A new calorimeter structure

A novel way of electron detection in compensating calorimeters is illustrated in fig.1. Consider a compensating structure of d_{Pb}/d_{Sc}=4:1 as in fig.1a. By decreasing the thickness of the absorber layers by a factor of 2 (see fig.1b) and inserting *additional layers of sensitive material* one can improve the energy resolution for electrons. If these additional layers do not contain hydrogen, i.e. the materials are inorganic, they should not affect the neutron component of the hadronic shower. With independent readout of the organic scintillators and the inorganic sensitive layers one has effectively two calorimeters allowing each shower to be sampled twice. The organic scintillators provide the compensating calorimeter for hadrons, while the inorganic plus organic sensitive layers provide the signal for electrons with an improved energy resolution without affecting the hadron detection.

The sensitive layers can be in the form of tiles as in fig.1 or in the form of fibers as in spaghetti calorimeters. The relative signals of the calorimeters can be set so that the signals from monoenergetic electrons are equal. The calorimeter formed with the inorganic fibers/tiles should be undercompensating ($e/h > 1$) so that the difference between the signals of the two calorimeters is large for hadrons. This provides additional information for the separation of electrons from hadrons.

Various designs can be considered. The spaghetti structure seems to be well suited for the purpose. The additional fibers can be of any inorganic scintillating material, e.g. glass fibers; although their efficiency of detection of ionization is lower than that of plastic fibers, this is compensated by the larger energy deposition in the denser material. Quartz fibers sensitive to Čerenkov light[18] are good candidates if they are radiation hard. Sacrificing on uniformity one can investigate a calorimeter structure with the inorganic sensitive layers in the electromagnetic part of the calorimeter only and compensate for this with modified absorber plates in the hadronic section. Silicon detectors can be used although the need to support the silicon leads to rather large sampling gaps ($\sim$ 2 mm [15]). One can also replace the lead absorber plates with dense scintillating crystals, e.g. PbF_2; the crystals serve as the active medium for electron detection and the passive for hadrons. The observed progress in the technology of detector designs suggests that better solutions could be provided in the near future.

3. Monte Carlo investigations

The influence of *additional layers* of material on hadron and electron detection in the lead-organic scintillator compensating calorimeters has been investigated with Monte Carlo codes. First the published results of hadron shower simulations [10] have been reexamined to study the sensitivity of hadronic shower characteristics to additional lead layers. Then these studies are extended to other materials using the same code. The sensitivity of the electron detection has been investigated with the EGS4 code[19]. The aim of these Monte Carlo studies is to

indicate qualitative changes in the hadron and electron detection in the modified compensating calorimeters.

One can expect that the shower development is similar in the two geometrical configurations used for sampling calorimeters: a sandwich structure with layers perpendicular to the beam direction and a spaghetti structure with fibers nearly parallel to the beam direction. For simplicity only the sandwich structure, as shown in fig.1, is considered.

3.1. Lead-scintillator calorimeters

Hadron detection in lead-organic scintillator (Pb/Sc) calorimeters has been investigated [10] using the FLUKA90 code[20] which includes low energy neutron transport [21]. Predictions have been compared with experimental data for a wide range of calorimeter structures with the relative thickness of lead to scintillator between 0 and 8 and at incident energies between 5 and 200 GeV. Good agreement within the experimental errors is found. As part of these studies hadronic showers have also been simulated in infinitely large Pb/Sc calorimeters for two thicknesses of scintillator plates, 0.10 and 0.25cm, and with the thickness of the lead plates in the range from 0.1 to 3.5cm. The obtained values of the e/h ratio and the total energy resolution show that compensation is achieved for a relative volume of absorber to active media of 4:1, but 3:1 and 5:1 are still acceptable, depending on the incident energy.

A simplified description of hadronic shower detection can be made by subdividing the 'deposited' energy into components which are characterized by the same detection features. The main components are ionization due to electrons (the electromagnetic component E_{ele}), ionization due to charged hadrons E_{ch} and the energy carried by neutrons emitted with kinetic energy below 20 MeV E_{neu}. The contribution of each component to the calorimeter signal S is given by its corresponding detection efficiency α leading to the following approximation of the hadron signal:

$$S = \alpha_{ele} \cdot E_{ele} + \alpha_{ch} \cdot E_{ch} + \alpha_{neu} \cdot E_{neu} + \epsilon,$$

where ϵ represents a correction from other components simulated by the Monte Carlo model. The average energy deposited by each component for 10 GeV π^- showers is shown in fig.2 as a function of the ratio of the thicknesses of the absorber to scintillator layers, d_{Pb}/d_{Sc}. In fig.3 the average number of hadron interactions in the showers are shown in the lead layers and in the scintillator. One can see that for $3 \leq d_{Pb}/d_{Sc} \leq 5$, i.e. around the compensating structure, the hadronic shower development is determined by the interactions in the lead.

3.2. Calorimeters with additional layers

In order to investigate the influence of additional layers of material on hadron and electron detection Monte Carlo studies have been carried out for the calorimeter structure shown in fig.1b with additional layers consisting of magnesium, aluminum and iron. The neutron transport for these materials is provided for in the modified FLUKA90 code [21]. The results are presented in figs 4-8 as a function of the density of the material in the additional layers. They are based on samples of 3000 showers produced by 10 GeV π^- and 600 showers produced by 10 GeV e^-. For comparison, results are included for the cases when no additional material is added and when the material in the additional layers is organic scintillator or lead.

Fig.4 shows that the average energy deposited by the hadronic shower components is weakly modified by interactions in additional layers although the interactions contribute to the shower development in heavier materials like iron (fig.5). The detection efficiencies α are strongly changed if the layers contain hydrogen as is the case when the additional organic scintillators are added (fig.6). As expected, only the material with some hydrogen content affects the calorimeter energy resolution for hadrons (fig.7).

The degradation of the energy resolution caused by the additional hydrogenous material, shown in fig.7, is more apparent than in the measurements [8, 9] described in section 1.2. This comes from the fact that the response of the experimentally investigated calorimeters is dominated by sampling fluctuations [8, 10]. Recall that the neutron detection contributes mainly to the intrinsic fluctuations. Therefore the change in the measured energy resolution as a result of the structural changes is expected to be less than 10% at the investigated incident energies.

Electron detection is simulated using the EGS4 code[19]. The energy cutoff parameters and step sizes are set to the recommended values for sampling calorimeter structures (see e.g. [17]). It is found that the change in the 10 GeV electron signal detected by the organic scintillators is consistent with that expected from the increase of the absorber material (fig.6).

The e/h ratio is affected by the additional layers (fig.8). The increase of the thickness of the iron plates results in an increase in the e/h ratio, deviations of the hadronic signal distribution from the Gaussian shape as well as a degradation of the hadron energy resolution as have been measured in U/Cu/Sc calorimeters [1]. The changes in the energy resolution suggest that an acceptably good energy resolution can still be provided by a calorimeter built of dense scintillators interleaved with organic scintillators. Lead fluoride crystals are good candidates either as Čerenkov radiators or as scintillators; they have already been tested for electromagnetic calorimetry [13, 22].

The calorimeter structures discussed in this paper permit different components of the hadronic shower to be sampled by the organic and inorganic detectors; it may be possible to improve the hadron energy resolution by weighting these signals, online or offline, in a way similar to the method proposed in [23] (see also [22]). A Monte Carlo investigation of this method is in progress.

A number of issues need further Monte Carlo study. Notice however that Monte Carlo predictions for calorimeters with heavy absorbers ($A > 200$) are sensitive to assumptions on the spectra and transport of low-energy particles produced in electromagnetic and hadronic showers, e.g. photons and hadrons with energies of tens MeV or less and evaporation neutrons. Some features can change drastically from one material to another although the materials have similar A and Z. An optimization of the material parameters has not yet been done.

One can conclude that a moderate admixture of additional material in existing compensating calorimeters would not affect the hadron energy resolution if these layers do not contain hydrogen. They cause a decrease of the calorimeter signal for electrons and hadrons; an optimization is required to obtain compensating structures for hadron detection.

4. Conclusions

A possible way to improve the energy resolution for electromagnetic shower in compensating hadronic calorimeters is to add sensitive layers for the electromagnetic detection. Therefore, we suggest to install layers of inorganic active media in compensating calorimeters in such a way that one has effectively two calorimeters. Independent readout of the organic and inorganic active

media allows for compensation and good energy resolution for hadrons, and the improvement of the energy measurement for electrons. The difference between the signals can be used for the separation of electrons from hadrons. Another feature of this structure is its capability to provide information for further use on showers originating from electromagnetic particles like electrons and on those components of hadronic showers which are detected in the inorganic active medium. Balancing costs and particle detection the double spaghetti structure with lead as absorber and with organic and inorganic fibers as active media offers a good choice of calorimeter design for both electron and hadron detection.

Acknowledgments

The author wishes to thank the DESY directorate for financial support. The author is indebted to A.Dwurazny, D.Kisielewska, R.Klanner, G.Levman and M.Lomperski; this paper benefits from their suggestions.

References

[1] T.Akesson et al., Nucl. Inst. and Meth. A241(1985)17.

[2] G.d'Agostini et al., Nucl. Inst. and Meth. A274(1989)134.

[3] E.Bernardi et al., Nucl. Inst. and Meth. A262(1987)229.

[4] D.Acosta et al., Nucl. Inst. and Meth. A308(1991)481.

[5] B.Anders et al., DESY 86-105, 1986.
M.G.Catanesi et al., Nucl. Inst. and Meth. A260(1987)43.
Y.Galaktionov et al., Nucl. Inst. and Meth. A251(1986)258.
J.Engler et al., Nucl. Inst. and Meth. A320(1992)460.

[6] R.Wigmans, Nucl. Inst. and Meth. A259(1987)389.
H.Brückmann, U.Behrens, B.Anders, Nucl. Inst. Meth. A263(1988)136.
J.E.Brau, T.Gabriel, Nucl. Inst. and Meth., A279(1989)40.
P.K.Job et al., Nucl. Inst. and Meth. A309(1991)60.

[7] P.K.Job et al., Nucl. Inst. and Meth. A340(1994)283.

[8] G.Drews et al., Nucl. Inst. and Meth. A290(1990)335.

[9] A.Tsirou, *On the Optimization of a Lead-Scintillator Compensating Calorimeter*, Ph.D. Thesis, University of Wisconsin-Madison, 1989.

[10] T.Tymieniecka, Nucl. Inst. and Meth. A336(1993)442.

[11] J.Bakken et al., Nucl. Inst. and Meth. A254(1987)535.
B.Adeva et al., Nucl. Inst. and Meth. A289(1990)35.

[12] K.Ahmet et al., Nucl. Inst. and Meth. A305(1991)275.

[13] R.D.Appuhn et al., DESY 93-143, 1993.

[14] J.Badier et al., Nucl. Inst. and Meth. A337(1993)314.

[15] M.Bosetti et al., Nucl. Inst. and Meth. A345(1994)244.
E.Borchi et al., Nucl. Inst. and Meth. A279(1989)57.

[16] B.Aubert et al., Nucl. Inst. and Meth. A334(1993)383.

[17] J. del Peso, E. Ros, Nucl. Inst. and Meth. A276(1989)456.

[18] K.Johnson, *Very forward calorimetry with quartz fibers excited by Čerenkov light*, The Fourth International Conference on Calorimetry In High Energy Physics, La Biodola, Isola d'Elba, Sept.,19-25, 1993, ed. A. Menzione.

[19] W.R.Nelson,H.Hirayama,D.O.Rogers, SLAC-265(1985).

[20] P.A.Aarnio, H.J.Möhring, J.Ranft, A.Fasso, G.R.Stevenson,
FLUKA89 Users' Guide, CERN TIS-RP Divisional Report, 1989.

[21] J.M.Zazula, DESY-D3-66, 1990.

[22] D.F.Anderson, E.J.Ramberg, *Recent Developments in High-Speed Non-Sampling Electromagnetic Calorimetry*, Proceedings of the 5th International Conf. on Instrumentation for Colliding Beam Physics, Novosibirsk, USSR, 1990. Novosibirsk Instrument Workshop, 1990:290-298(QCD201:I5:1990).

[23] H.Abramowicz et al., Nucl. Inst. and Meth. 180(1981)429.

Figure Captions

Fig.1 For simplicity calorimeters are shown with a multilayer 'sandwich' structure with layers perpendicular to the beam direction:
(a) a compensating Pb/Sc calorimeter with the thickness of the lead absorber plates d_{Pb}=4 mm and with the thickness of the scintillator plates d_{Sc} equal to 1 mm;
(b) a Pb/Sc/X calorimeter as in (a) but with every lead plate divided into two and material layer X of 1mm thickness implemented in-between.

Fig.2 Monte Carlo estimates of the average energy deposited by 10 GeV π^- showers in lead-organic scintillator calorimeter plotted as a function of the ratio of the thicknesses of the absorber and scintillator layers, d_{Pb}/d_{Sc}. The values for three components are plotted: the ionization due to electrons (E_{ele}), the ionization due to charged hadrons (E_{ch}) and the energy carried by neutrons (E_{neu}). The estimates presented as open symbols are taken from the simulations described in [10]. The lines are drawn to guide the eye.

Fig.3 As fig. 2 showing the average number of hadron interactions per shower in the lead and in the scintillator. An interaction in a hadronic shower is counted if the interacting hadron has a kinetic energy above 50 MeV (the FLUKA convention).

Fig.4 Monte Carlo estimates of the average energy deposited by 10 GeV π^- showers in Pb/Sc/X calorimeters (shown in fig.1b) plotted as a function of the density of the material used in the layers X. Three components of hadronic showers are plotted: the ionization due to electrons (E_{ele}), the ionization due to charged hadrons (E_{ch}) and the energy carried by neutrons (E_{neu}). The estimates presented as open symbols are taken from the simulations described in [10]. The lines are drawn to guide the eye. Results are shown for the structure with no additional material (indicated with an arrow) and with additional materials X of organic scintillator (Sc), magnesium, aluminum, iron and lead.

Fig.5 As fig. 4 showing the average number of interactions per shower in lead, in scintillator and in the additional material X. An interaction in a hadronic shower is counted if the interacting hadron has a kinetic energy above 50 MeV (the FLUKA convention).

Fig.6 As fig.4 showing the detection efficiency α in Pb/Sc/X calorimeters for three components of hadronic showers: the ionization due to charged hadrons (α_{ch}), the ionization due to electrons (α_{ele}) and the energy carried by neutrons (α_{neu}).

Fig.7 The energy resolution $\sigma_E/E \cdot \sqrt{E}$ for Pb/Sc/X calorimeters plotted as a function of the density of the material. The estimates are done for 10 GeV showers. The estimates presented as open symbols are taken from the simulations described in [10]. The lines are drawn to guide the eye. Results are shown for the structure with no additional material (indicated with an arrow) and with additional materials X of organic scintillator (Sc), magnesium, aluminum, iron and lead.

Fig.8 As fig.7 showing the e/h-ratio for the Pb/Sc/X calorimeters.

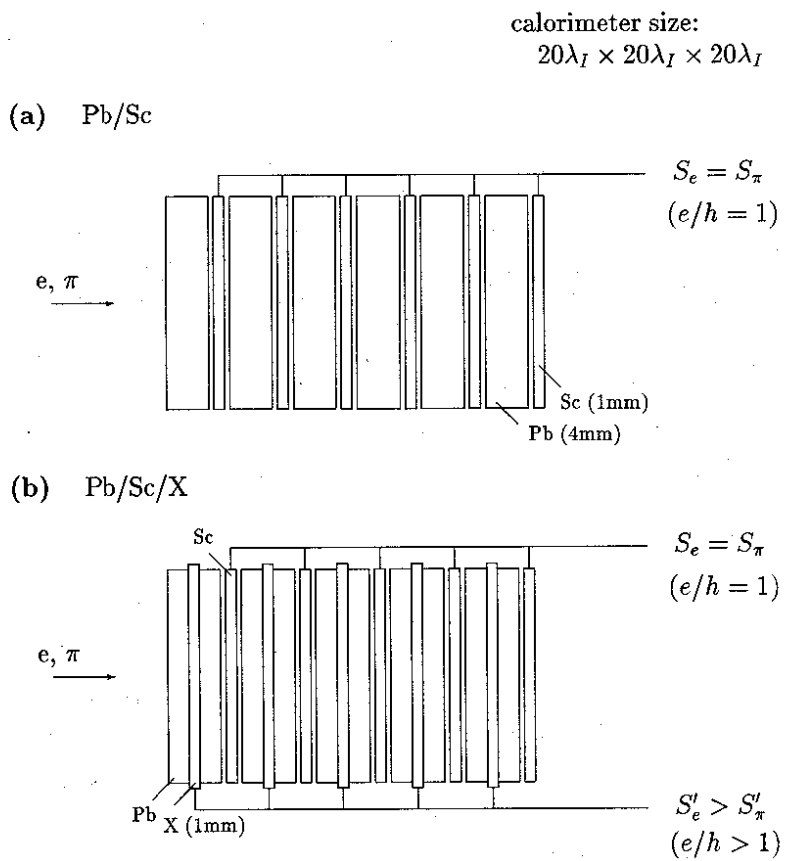

Figure 1: For simplicity of illustration calorimeters are shown with a multilayer 'sandwich' structure with layers perpendicular to the beam direction:
(a) a compensating Pb/Sc calorimeter with the thickness of the lead absorber plates d_{Pb}=4 mm and with the thickness of scintillator plates d_{Sc} equal to 1 mm;
(b) a Pb/Sc/X calorimeter as in (a) but every lead plate is divided into two plates and an extra material layer X of 1mm thickness is implemented in-between.

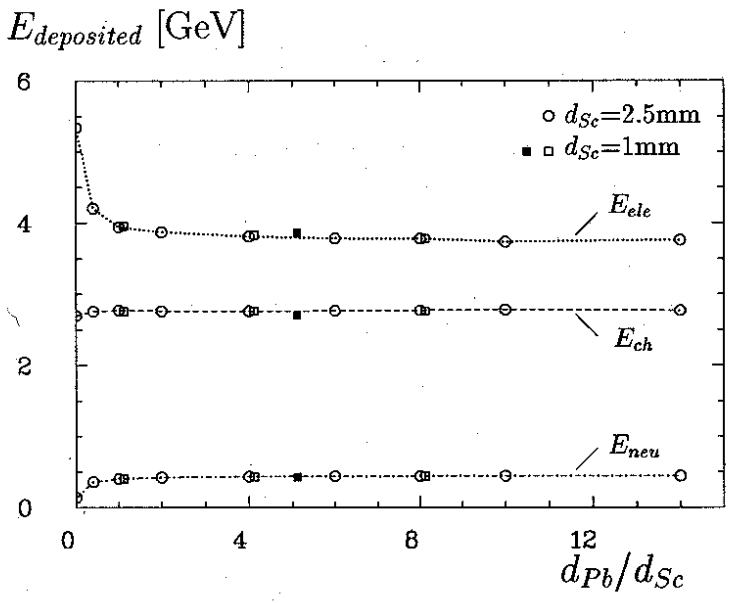

Figure 2: Monte Carlo estimates of the mean energy 'deposited' (see text) in lead-organic scintillator calorimeter for a 10 GeV π^- shower plotted as a function of the ratio of the thicknesses of the absorber and scintillator layers, d_{Pb}/d_{Sc}. Three components of hadronic shower are plotted: the ionization due to electrons (E_{ele}), the ionization due to charged hadrons (E_{ch}) and the energy carried by neutrons (E_{neu}). The estimates presented as open symbols are taken from simulations described in [10]. The lines are drawn to guide the eye.

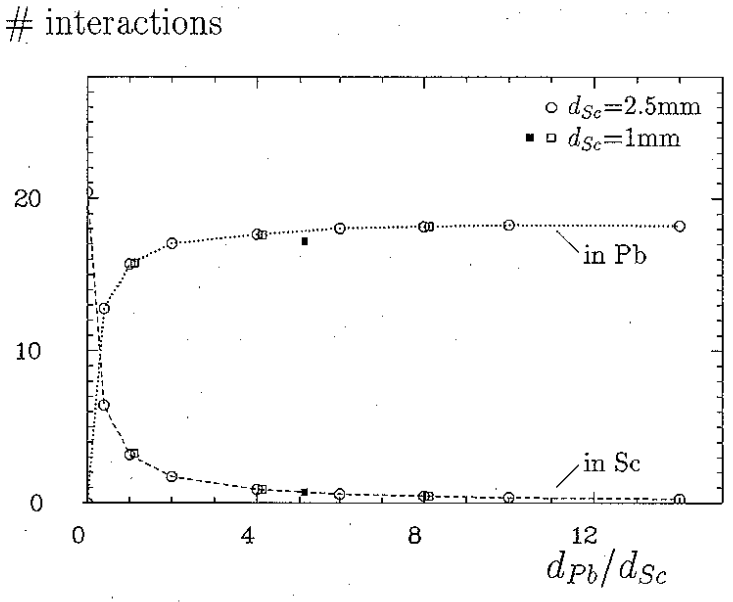

Figure 3: As in fig. 2 but the number of interactions per shower in lead and in scintillator are plotted. An interaction in a hadronic shower is counted if the interacting hadron has a kinetic energy above 50 MeV (the FLUKA convention).

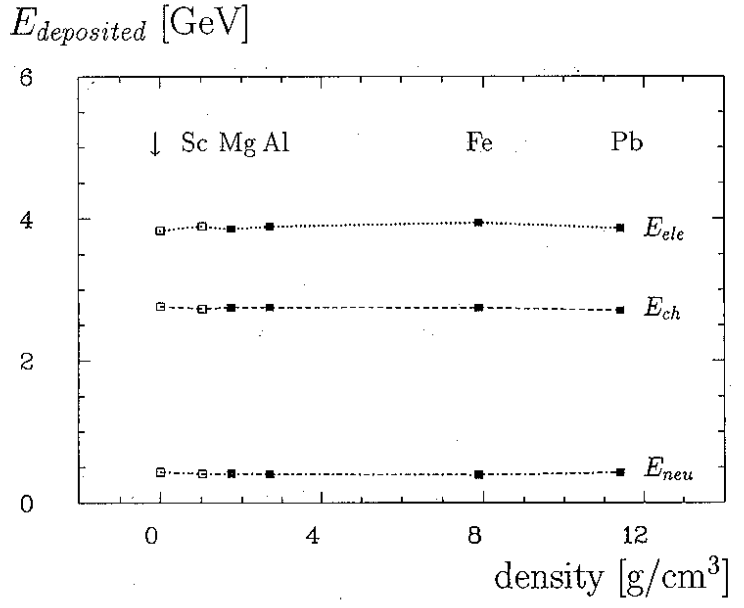

Figure 4: Monte Carlo estimates of the mean energy 'deposited' (see text) in the Pb/Sc/X calorimeters (shown in fig.1b) for a 10 GeV π^- shower plotted as a function of the density of material used in the extra layers X. Three components of hadronic shower are plotted: the ionization due to electrons (E_{ele}), the ionization due to charged hadrons (E_{ch}) and the energy carried by neutrons (E_{neu}). The estimates presented as open symbols are taken from the simulations described in [10]. The lines are drawn to guide the eye. The arrow marks the structure with no extra materials, Sc denotes the extra layers of organic scintillators and then Mg, Al, Fe and Pb are shown respectively.

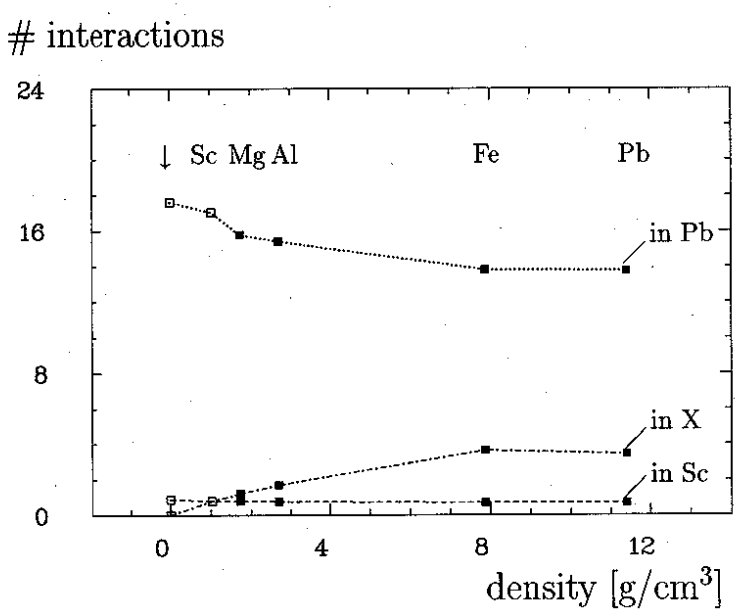

Figure 5: As in fig. 4 but the number of interactions per shower in lead, in scintillator and in the extra material X are plotted. An interaction in a hadronic shower is counted if the interacting hadron has a kinetic energy above 50 MeV (the FLUKA convention).

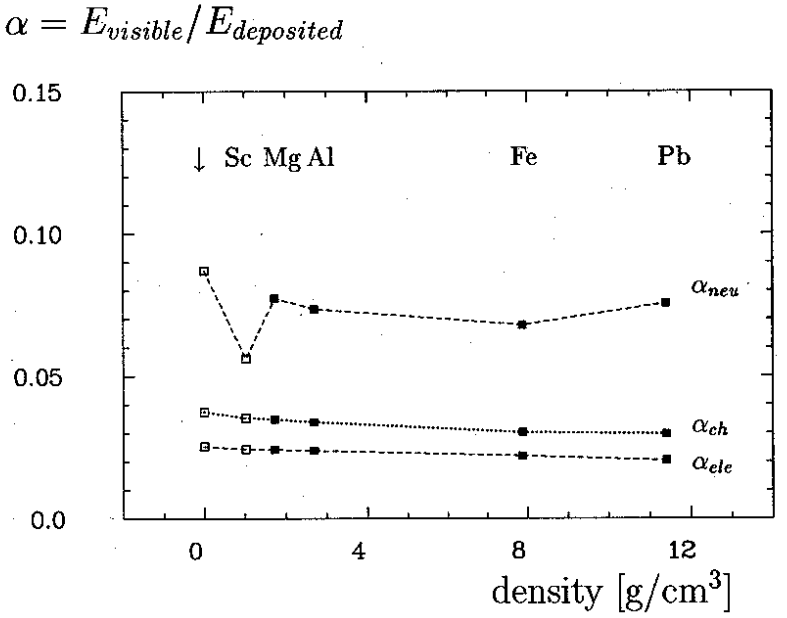

Figure 6: As in fig.4 but the detection efficiency α in Pb/Sc/X calorimeters is plotted for three components of hadronic shower: for the ionization due to charged hadrons (α_{ch}), for the ionization due to electrons (α_{ele}) and for the energy carried by neutrons (α_{neu}).

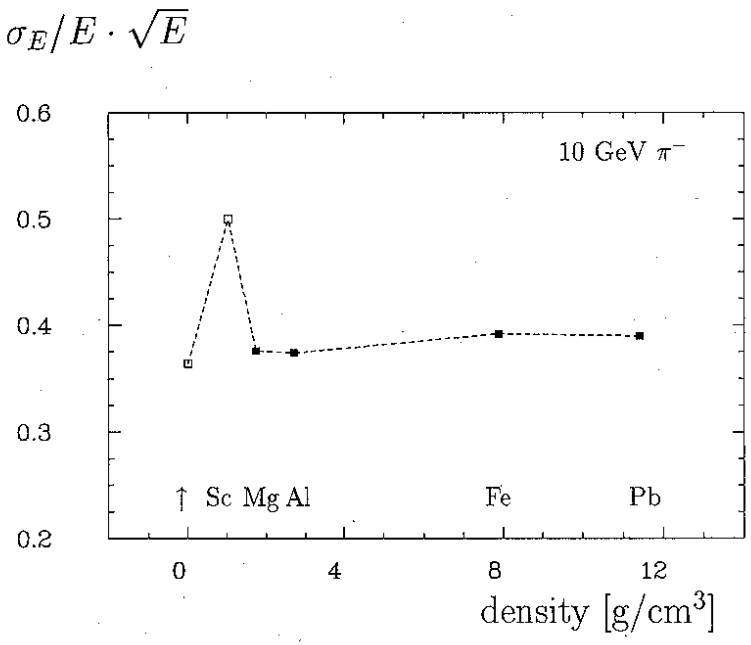

Figure 7: The energy resolution $\sigma_E/E \cdot \sqrt{E}$ for the Pb/Sc/X calorimeters plotted as a function of the density of material used in the extra layers X. The estimates are done for 10 GeV showers. The estimates presented as open symbols are taken from the simulations described in [10]. The lines are drawn to guide the eye. The arrow marks the structure with no extra materials, Sc denotes the extra layers of organic scintillators and then Mg, Al, Fe and Pb are shown respectively.

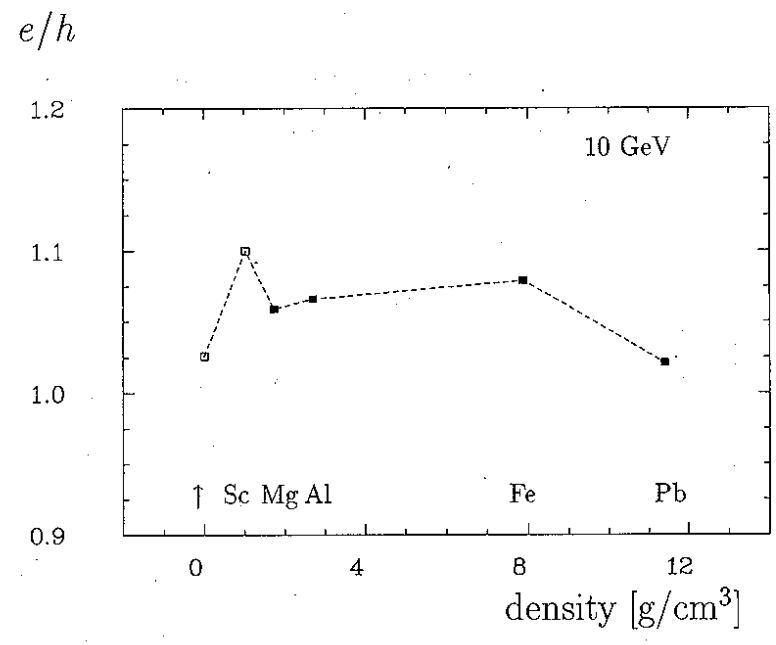

Figure 8: As in fig.7 but the e/h-ratio for the Pb/Sc/X calorimeters are plotted.